Supported Palladium Catalysts for the Conversion of Furfural with Polymethylhydrosiloxane

M. Esther Medina Ruiz,[†] Rocío Maderuelo-Solera,[†] Carmen P. Jiménez-Gómez,[†] Ramón Moreno-Tost,[†] Irene Malpartida,[‡] Cristina García-Sancho,[†] Juan Antonio Cecilia,[†] Christophe Len,[§,||,*] Josefa M. Mérida-Robles,[†,*] Pedro Maireles-Torres,[†]

[†] *Universidad de Málaga, Departamento de Química Inorgánica, Cristalografía y Mineralogía, Facultad de Ciencias, Campus de Teatinos, 29071, Málaga, Spain*

[‡] *Deasyl S.A., Plan-les-Ouates, Geneva, 1228, Switzerland*

[§] *Chimie ParisTech, PSL Research University, CNRS, Institute of Chemistry for Life and Health Sciences (i-CLeHS), 11 Rue Pierre et Marie Curie, F-75005 Paris, France*

[||] *Sorbonne Universités, Université de Technologie de Compiègne, F-60200, Compiégne, France*

Corresponding author: christophe.len@chimieparistech.psl.eu; jmerida@uma.es

ABSTRACT: A series of Pd-based catalysts supported on oxidic materials with different acid-base properties has been prepared, characterized and used for the valorization of furfural into value-added chemicals, with polymethylhydroxysiloxane (PMHS) as reducing agent as alternative to the use of hydrogen gas and alcohols as hydrogen donors. PMHS is a polymeric waste product of the silicone industry, being also recognized as a sustainable reductant for epoxide hydrosilylations and diastereoselective radical reduction in organic chemistry. Moreover, it is non-toxic, water/air insensitive and soluble in most organic solvents due to its low viscosity. So, PMHS has been employed

Comentado [RMT1]: Indicar a qué

Comentado [RMT2]: NO es necesario

for the reduction of furfural in the presence of supported Pd catalysts. Although all catalysts tested are catalytically active, those supported on Al_2O_3 and SiO_2 showed complete conversion after 30 min of reaction at 303 K, whereas a 27.7% was attained using MgO. $1PdAl_2O_3$ (1 wt% Pd) catalyst was initially very selective to furfuryl alcohol (80.4% yield of FOL), which was hydrogenated to tetrahydrofurfuryl alcohol (THFA) at longer reaction times, reaching yields of 48.8 and 33.4% of FOL and THFA, respectively, after 6 h. By increasing the amount of Pd until 5 wt%, the reaction evolves towards the formation of more hydrogenated products (THFA), although the amount of non-detected products also increases. The best FOL productivity data has been achieved with $1PdAl_2O_3$, which attained a TOF value of 397 h^{-1} (mol_{FOL} mol_{Pd}^{-1} h^{-1}) at 303 K after only 30 minutes, with only 180 μL of PMHS in ethanol, as solvent, while increasing both the amount of Pd to 2.5 wt% ($2.5PdAl_2O_3$) and that of PMHS until 360 μL, under similar experimental conditions, 100 mol_{THFA} mol_{Pd}^{-1} h^{-1} can be produced.

KERWORDS: Polymethylhydrosiloxane, Furfural, Biomass, Palladium, Heterogeneous catalysis

INTRODUCTION

The transition from an economy based on fossil resources to one based on renewable alternatives is one of the great challenges facing society today. The escalating demand for energy and chemicals, driving by the rapid development of the economy and population growth has drawn considerable attention to the search for sustainable and renewable raw materials. Lignocellulosic biomass stands out at the most abundant source, not only of energy and biofuels, such as biodiesel and ethanol[1], but also of various other valuable carbon-based chemicals[2]. Consequently, cellulose and hemicellulose, the primary natural source of carbohydrates founds in lignocellulose, can undergo hydrolysis and subsequence reactions to yield numerous platform chemicals. Among them, furfural (FUR) holds significant potential for biofuels and chemical production[3].

Currently, the primary product obtained on a commercial scale from FUR is furfuryl alcohol (FOL). Additionally, tetrahydrofuran (THF), maleic anhydride, 2-methyltetrahydrofuran (MTHF) and 1,5-pentanediol are also noteworthy products with interesting applications.[4] Specifically, the reductive upgrading of FUR results in the entire class of furan-based chemicals, including FOL, THF and MTHF, as mentioned earlier[5–7].

The selective hydrogenation of the formyl group is the most extensively studied process, as approximately 62% of FUR is industrially used to produce FOL.[8] FOL finds application in the production of furan resins, fine chemicals, lysine, vitamin C, lubricants, dispersing agents, plasticizers, and in the synthesis of fibers.[9] Other compounds, such as levulinic acid (LA),[10] levulinic esters,[11] furfuryl ethers[12] and the intermediate for the synthesis of the anti-ulcer drug ranitidine,[3]can be prepared from FOL.

FOL can be transformed into other furan derivatives of interest, such as tetrahydrofurfuryl alcohol (THFOL), considered as a green solvent,[13] and a precursor to

Con formato: Fuente: Sin Negrita

Comentado [RMT3]: En el abstract pone THFA

diols, like 1,5-pentanediol, — a monomer used in the roduction of polyester or polyurethane.[14] FOL can also undergo conversion into MF and MTHF, which, aside from serving as solvents, exibit promise as fuel additives due to their high energy density, elevated octane number, and hydrophobicity.[15] Furthermore, the hydrogenation of FOL followed by subsequent isomerization, produces a crucial intermediate for the synthesis of insecticides and rubber chemicals (cyclopentanone).[16]

FUR demonstrates excellent hydrogenation reactivity under high-pressure of H_2 conditions, with heterogeneous catalytic systems utilizing noble metals (Pt, Ru, Pd, Ag, etc.) or non-noble metals (Cu, Fe, Ni, etc.) in both gas and liquid phases.[3,17] Catalysts based on noble metals generally exhibit higher activity under milder reaction conditions than those based on non-noble metals, and are more selective toward deep hydrogenated products, such as THFOL and MTHF. To enhance catalytic processes relying on noble metals, optimization studies are necessary to minimize the use of noble metal, due to their scarcity and high cost, while improving recyclability. Additionally, safety concerns and the high cost of H_2 gas have spurred investigations into more economical and safer hydrogen sources. A widely explored alternative is catalytic transfer hydrogenation (CTH), with numerous studies focused on the reductive upgrading of FUR through CTH, many employing short-chain aliphatic alcohols that are cost-effective, easy to handle, and derived directly from biomass, serving as suitable hydrogen donors.[18,19] Consequently, transfer hydrogenation using organic alcohols emerges as a more environmentally friendly method compared to conventional hydrogenation processes using H_2 gas. In recent years, extensive research has been conducted on CTH of furfural in the presence of aliphatic alcohols using single-metal and bimetallic catalysts based on both noble [3,20,21] and non-noble metals.[5,20]

Comentado [RMT4]: Lo mismo que antes

On the other hand, the primary drawbacks associated with the use of aliphatic alcohols in CTH include the formation of the oxidation product of the alcohol, used as H-donor/solvent, and the reaction of the alcohol with FOL through etherification under the harsh conditions employed. These reactions ultimately diminish the selectivity of the CTH process.[22] Consequently, alternative hydrogen donors have been explored to address these challenges. Formic acid has been extensively investigated as an H-donor due to its sustainable production from carbohydrates, offering the advantage that CO_2 is the only secondary product.[23] However, despite the high FOL yields (99%) achieved with bimetallic-based catalysts, such as Cu-Pd/C[24] or $Cu/MgAl_2O_4$,[25] when using formic acid as an H-donor, the use of this acid can lead to corrosion problems in the equipment.

Polymethylhydrosiloxane (Me_3Si-$(OSiMeH)_nOSiMe_3$, PMHS) is a promising chemical for use as a hydrogenating agent, as the Si-H bonds can be activated under mild conditions.[26] PMHS is inexpensive and abundant, being a by-product of the silicone industry. It is non-toxic, water/air insensitive and soluble in most organic solvents due to its low viscosity. Therefore, KF was used to catalyze the hydrogenation of FUR and 5-hydroxymethylfurfural to FOL and 2,5-bis(hydroxymethyl)furan, respectively, with high yields (97% and 98%, respectively).[27,28] Furthermore, this salt was impregnated on ZrO_2 to obtain a KF/ZrO_2 catalyst, which produced a 97% FOL yield at 99% FUR conversion, at 25 ºC after 0.5 h of the reaction, using PMHS as H-donor and high polar aprotic solvents such as dimethyl sulfoxide or *N*,*N*-dimethylformamide. Protonic solvents displayed lower FOL yield, due to the negative effect of H-bonding on the nucleophilicity of the fluoride ion. After five cycles of the reaction, FOL yield fell to 71%, attributed to pore coverage by PMHS-based resins.[29] FUR was also selectively converted to FOL (81%-99% yield) using another alkaline salt, Cs_2CO_3, as catalyst, and PMHS as hydrogen source at 298-353 K in 2-6 h. However, the interaction of carbonate with hydrosiloxane

facilitated the formation of silicon formate, leading to asignificant decrease in catalytic activity in the reused catalyst.[30] When tetraethylammonium fluoride and PMHS were used in the catalytic transformation of FUR, it was claimed that the fluoride-activated hydrosilylation was responsible for the efficient transfer hydrogenation process. After reacting at 308 K for 0.5 h, a FUR conversion of 94.9% and a FOL yield of 92.3% could be achieved.[31]

Pd-based catalysts have also been studied for the hydrogenation of FUR, using PMHS as H-donor. Commercial Pd/C catalysts and PMHS were found to be active in selective hydrogenation along with cascade reactions, leading to the efficient conversion of FUR into different value-added chemicals, such as FOL, MF and THFOL, with yields ≥90%. This was achieved after optimization various reaction parameters, such as temperature (288-373 K), PMHS dosage (2-4 equiv. H^-), type of acid sites (Brönsted or Lewis) and dopant water content (10%-70% by weight).[32] Regarding the selective conversion of FUR in FOL, a long reaction time (12 h) was required. Pd nanoparticles supported on metal organic frameworks (Pd/MOFs) catalysts were used for the transformation of carbohydrates and a variety of biomass-derived products, using PMHS as an H-donor. FUR was completely converted with a 97% yield to MF at 298 K and 120 min of reaction in n-butanol.[33] Ding et al. recently developed an efficient Pd-Zr-HZSM-5 catalyst for the selective HDO of bio-based ketones and aldehydes, using PMHS as an H-donor. Particularly for FUR reaction, a conversion >99% and a selectivity towards FOL of 93.6% were obtained using ethanol as solvent, after 3 h of reaction at 308 K.[34] The authors related the abundance of oxygen vacancies in the catalyst to the high dissociation of silane into H^+, avoiding the use of acid additives and resulting in a catalyst that could be reused in at least six reaction cycles.

Con formato: Resaltar

The use of PMHS as a green H-donor molecule to replace molecular H_2 in biomass hydrodeoxygenation reactions under mild conditions still needs to be optimized, especially regarding selectivity towards the desired reaction product. Therefore, in the present work, the use of different metal oxides as support to obtain Pd-based catalysts for the selective hydrogenation of FUR under mild conditions has been performed. The role of the acid-base nature of the support in the selective transformation of FUR was analysed by optimizing different reaction parameters.

EXPEIMENTAL SECTION

Material. Furfural (99%) was purchased from Sigma-Aldrich. In addition, $PdCl_2$ (Pressure Chemical Co.), HCl (VWR), SiO_2 (Sigma-Aldrich), Al_2O_3 (VWR) and MgO (Sigma-Aldrich) were also used. These products were used directly as received without further purification.

Catalyst Preparation. Pd-based catalysts were synthesized from $PdCl_2$ dissolved in HCl to obtain a 0.01 M solution of H_2PdCl_4. This acid solution was then used to incorporate Pd species onto various commercial supports, such as SiO_2, Al_2O_3 and MgO, by incipient wetness impregnation, with a Pd content ranging between 1 and 5 wt% for all supports. After incipient wet impregnation, the catalysts were dried at 80 °C overnight and calcined at 400 °C for 2 h, at a heating rate of 2 °C min^{-1}. Catalysts were labeled as xPd support, where x is the weight percent of Pd incorporated to each support.

Catalyst Characterization. An X-Pert Pro automated diffractometer equipped with a Ge (111) primary monochromator with Cu K α1 radiation and an X'Celerator detector with a step size of 0.017º was used to obtain power X-ray diffraction patterns. Data was collected from 10º to 70º in 2θ for a total counting time of 712 s per step. The crystallite

size was then calculated using the Williamson-Hall equation, where θ is the Bragg angle, B is the full width at half maximum (FWHM) of the XRD peaks, K is the Scherrer constant, λ is the wavelength of the X-ray, and ε is the lattice strain.[35] The equation is written as: $B\cos\theta = (K\lambda/D) + (2\varepsilon\sin\theta)$.

N_2 adsorption-desorption isotherms at -196 ºC were measured using a Micromeritics Inc. ASAP 2420 model gas adsorption analyzer. Samples were outgassed overnight at 473 K and 10^{-4} mbar at a heating rate of 10 ºC min^{-1} prior to the N_2 sorption. The surface area of the sample was determined using the Brunauer-Emmett-Teller (BET) equation,[36] which assumes a nitrogen molecule cross section of 16.2 $Å^2$. The pore size distribution was calculated using density functional theory (DFT),[37] and the total pore volume was obtained from N_2 adsorption at a pressure ratio of P/P_0= 0.95.

The surface chemical composition of the catalysts was analyzed using X-ray photoelectron spectra (XPS) measurements with a Physical Electronics Model PHI 5701 spectrometer. The PHI ACCESS ESCA-V 6.0 F software was used to acquire spectra in constant pass energy mode at an energy of 29.35 eV. The binding energy (BE) was measured relative to the C 1 s peak from the adventitious contamination layer at 284.8 eV, with an estimated error of approximately 0.1 eV. The data was then analyzed using the Multipak v8.2b software. The purpose of the XPS measurements was to evaluate the surface chemical composition of the catalysts.

A TALOS Model F200x instrument, capable of both high-resolution transmission electron microscopy (HRTEM) and scanning electron microscopy (STEM) modes, was used to obtain HRTEM images for morphology and particle size distribution analysis. Microanalysis was performed using an EDX Super-X system with four X-ray detectors and an X-FEG beam.

Catalytic Studies. The furfural hydrogenation was carried out using glass pressure reactors with threaded bushings (Ace, 15 mL, pressure rated to 1 MPa). In the experiments, 50 mg of supported Pd catalysts, or 17 mg $PdCl_2$, were mixed with different amounts of furfural (96 and 288 µl), 5 mL of ethanol (EtOH) as solvent, and PMHS was used as a H-donor molecule to replace H_2. In all cases, the reactors were always purged with helium. The reaction time was extended from 30 min to 6 h, under continuous stirring (450 rpm), while the reaction temperature ranged between 303 and 333 K. The temperature was controlled by a thermocouple directly in contact with a steel block. At the end of the reaction, the reactor was removed from the steel block and cooled in a water bath. The samples were then filtered through a microfilter and analyzed using gas chromatography (Shimadzu GC-14A) equipped with a flame ionization detector and a CP-Wax 52 CB capillary column. The furfural conversion and selectivity were calculated from the data obtained as follows:

$$\text{Conversion (\%)} = \frac{\text{mol of furfural converted}}{\text{mol of furfural fed}} \times 100$$

$$\text{Selectivity (\%)} = \frac{\text{mol of the product}}{\text{mol of the furfural converted}} \times 100$$

RESULTS AND DISCUSSION

Catalytic performance. Under the experimental conditions used in this study, the reaction products detected were those shown in **Scheme 1**. Thus, FOL is formed by hydrogenation of C=O of FUR molecule, whereas THFA results from complete hydrogenation of the furan ring. MF is formed by C-O hydrogenolysis of FOL, while hydrogenation of the furan ring of MF leads to MTHF, which can also be produced by C-O hydrogenolysis of THFA.

Con formato: Resaltar

Scheme 1. Reaction pathways for hydrogenation/hydrodeoxygenation of FUR.

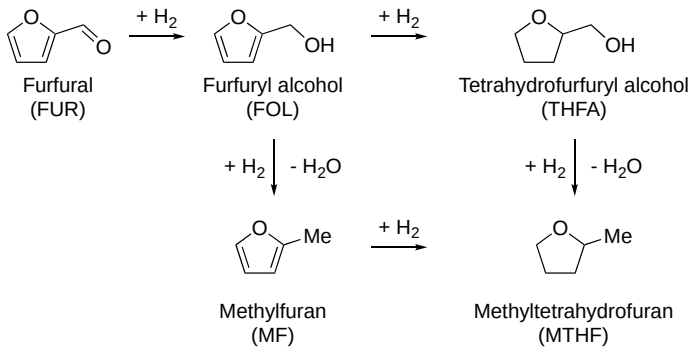

Comentado [RMT5]: No se ven las flechas y algunas moléculas no están completas

In addition, some experiments showed that small amounts of ethyl furfuryl ether were formed via etherification of FOL and ethanol, used as solvent.[38] Some previous studies have demonstrated the involvement of the solvent in competitive reactions leading to the formation of acetyl and/or ester adducts.[39–41] Nevertheless, it has not been possible to close the carbon balance of the hydrogenation process by considering only the mentioned reaction products. GC-MS studies have revealed the interaction of FUR and/or FOL with PMHS, as will be discussed in the following sections. This interaction leads us to an underestimation of such compounds in the final carbon balance, so they are referred to as 'undetected' in the text.

First, a comparative study of the catalytic behavior of supported Pd catalysts with 1 wt% loading (1PdAl_2O_3, 1PdMgO and 1PdSiO_2) was performed at 303 K for 30 min reaction time, and compared with an unsupported Pd catalyst (commercial $PdCl_2$). The results of this initial catalytic screening are shown in **Figure 1**. Full FUR conversion was achieved for all catalysts, except for the one supported on MgO (1PdMgO), which achieved only 27.7 % conversion.

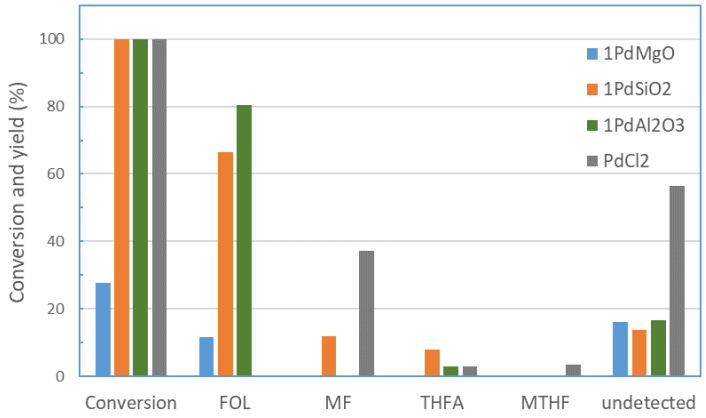

Figure 1. Hydrogenation of FUR with PMHS over a series of Pd-based catalysts. Experimental conditions: FUR (96 μL, 1.16 mmol), PMHS (180 μL), supported Pd catalyst (50 mg) or $PdCl_2$ (17 mg), ethanol (5 mL), 303 K, 30 min.

The selectivity pattern was very different for $PdCl_2$, where MF was the main product detected with a yield close to 40% and with a high amount of undetected products. For the supported Pd catalysts, the main reaction product was FOL, obtaining in all cases a much lower formation of undetected products (below 20% yield).

The selectivity pattern was very different for $PdCl_2$, where MF was the main product detected with a yield close to 40% and with a high amount of undetected products. For the supported Pd catalysts, the main reaction product was FOL, obtaining in all cases a much lower formation of undetected products (below 20% yield).

The results for the hydrogenation of FUR over supported Pd catalysts at different reaction times are shown in **Table 1**. Although all catalysts tested are catalytically active, those supported on Al_2O_3 and SiO_2 showed complete conversion after 30 min of reaction.

When MgO was used as support, only 27.7% conversion was obtained after 30 min of reaction, which increased with the reaction time, reaching 84.5% after 6 h.

Table 1. Hydrogenation of FUR with PMHS over supported Pd catalyst [a]

Catalyst	Time (min)	Conversion (%)	Yield (%)				
			FOL	THFA	MF	MTHF	Undetected
$1PdAl_2O_3$	30	100	80.4	3.0	0	0	16.6
	180	100	66.2	11.0	1.0	0	21.8
	360	100	48.8	33.4	2.5	0.8	14.5
$1PdSiO_2$	30	100	66.4	8.0	12.0	0	13.6
	180	100	37.5	16.8	24.5	0	21.2
	360	100	17.3	7.8	19.2	0	55.7
1PdMgO	30	27.7	11.6	0	0	0	16.1
	180	53.0	44.7	0	0	0	8.3
	360	84.5	56.1	0.8	0	0	27.6

[a] Experimental conditions: FUR (96 µL, 1.16 mmol), PMHS (180 µL), supported Pd catalyst (50 mg), ethanol (5 mL), 303 K, 30-360 min.

Regarding the yield to the different reaction products, $1PdAl_2O_3$ catalyst was initially very selective to FOL (80.4% yield), which was hydrogenated to THFA at longer reaction times, reaching yields of 48.8% and 33.4% for FOL and THFA, respectively, after 6 h.

Con formato: Resaltar

Con formato: Interlineado: sencillo

Con formato: Fuente: 12 pto

Con formato: Resaltar

Con formato: Resaltar

The formation MTMF was negligible and the amount of undetected compounds varied between 14.5% and 21.8%. The 1PdSiO$_2$ catalyst showed a very similar catalytic behavior to 1PdAl$_2$O$_3$, although it was slightly less selective to FOL due to its partial hydrogenolysis to MF, which reached a yield of 24.5% after 3 h of reaction. In addition, the percentage of undetected products was higher for this catalyst and increased with reaction time, reaching 55.7 % after 6 h of reaction. The 1PdMgO catalyst produced only FOL, but undetected products were also significant, especially after 6 h of reaction (27.3% yield).

By comparing the evolution the yields of the different reaction products for the different catalysts with the reaction time, it is possible to identify some possible reaction pathways for the hydrodeoxygenation of FUR in liquid phase. As shown in **Table 1**, FOL was the main reaction product at the beginning of the reaction, indicating that the hydrogenation of the C=O bond is favored over the hydrogenation of the furan ring. As reaction time increased, the consumption of FOL and the formation of were observed. In the case of 1PdAl$_2$O$_3$ catalyst, the decrease in FOL can be practically considered due to its hydrogenation to THFA with negligible production of MF or MTHF. However, for the 1PdSiO$_2$ catalyst, the increase in THFA production with reaction time was not parallel to the decrease in FOL production, indicating that there are other competitive reactions starting from FOL, in this case its hydrogenolysis to produce MF. This last reaction seems to be favorable up to 3 h, for higher reaction time a slight decrease in the production of MF can be observed and a large increase in the amount of undetected (55.7%) occurred.

In order to determine the influence of ~~palladium~~ Pd content on the catalytic performance, catalysts with 2.5 wt% and 5 wt% were also prepared using Al$_2$O$_3$ and SiO$_2$ as supports, and catalytic tests were carried out at 303 K. All catalysts showed complete FUR conversion (**Figure 2**). For the *x*PdAl$_2$O$_3$ catalysts, increasing the Pd content from

Comentado [RMT6]: Observado el qué?

Con formato: Resaltar

Con formato: Resaltar

1 to 2.5 wt% resulted in a drastic decrease in the yield to FOL (from 80% to 11.3%) in favor of THFA and MF, with yields of 23.4% and 36.7%, respectively. When the Pd content was increased to 5 wt% on Al_2O_3, the THFA yield reached 29% and the MF yield slightly decreased to 31.6% and small amounts of MTHF (3.4%) were also detected. These results show, as expected, that by increasing the Pd content, the hydrogenation power of the catalyst is higher, increasing the production of fully hydrogenated compounds such as THFA and MTHF. For the *x*$PdSiO_2$ catalysts, a very similar yield profile was observed for the catalysts with 1 wt% and 2.5 wt% Pd. Both catalysts, as previously discussed for 1$PdSiO_2$, produce THFA and MF in addition to FOL. When the Pd content was increased to 5 wt%, the yield to FOL decreased dramatically (9.4%) and the yield to THFA (11.9%) and especially to MF (52.9%) increased. An increase in the production of undetected products was also observed with palladium content for both series of catalysts.

Con formato: Resaltar

Con formato: Resaltar

Con formato: Resaltar

Con formato: Resaltar

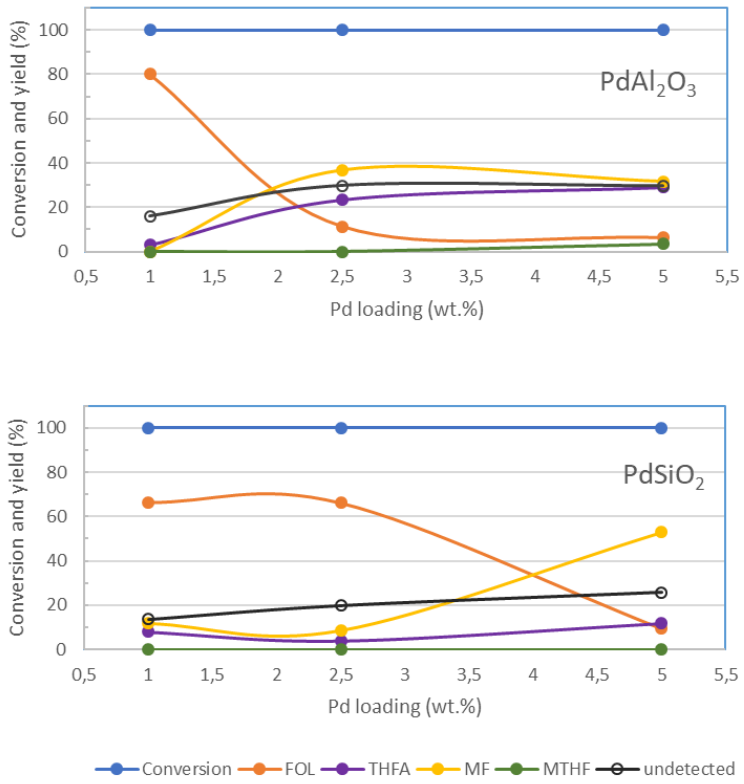

Figure 2. Effect of Pd loading on the hydrogenation of FUR with PMHS. Experimental conditions: FUR (96 μL, 1.16 mmol), PMHS (180 μL), supported Pd catalyst (50 mg), ethanol (5 mL), 303 K, 30 min.

Con formato: Justificado

These results allow us to conclude that both the nature of support and the Pd content significantly influence the selectivity towards the different reaction products. Thus, the catalysts with lower Pd contents ($1PdAl_2O_3$, $1PdSiO_2$) mainly produce FOL after 30 min of reaction, while for those with higher Pd contents ($5PdAl_2O_3$ and $5PdSiO_2$) evolve the reaction towards the total hydrogenation product of FUR (THFA) and towards the

Con formato: Resaltar

dehydrogenation product of FOL (MF). Medium (2.5 wt%) Pd loadings show intermediate behavior.

The effects of reaction temperature and FUR and PMHS dosage on the catalytic performance of $1PdAl_2O_3$ and $1PdSiO_2$ catalysts in FUR hydrogenation were also evaluated (**Table 2**). Conversions close to 100% were obtained for both catalysts at 303 K and 333 K (**Table 2, entries 1, 4, 6 and 9**), but the increase in temperature significantly affected the yield of the different reaction products. For the $1PdAl_2O_3$ catalyst, the yield of FOL decreased from 80.4% to 62.9% by increasing the reaction temperature from 303 K to 333 K, and in parallel a significant increase in undetected products was observed, from 16.6% to 33% (**Table 2, entries 1 and 4**). Similar behaviour was observed for the $1PdSiO_2$ catalyst. The yield to FOL, THFA and MF decreased at higher temperatures, while the percentage of undetected products increased from 13.6% to 28.7% (**Table 2, entries 6 and 9**). Therefore, it can be concluded that the best yields to FOL were obtained at low temperature (303 K), because higher temperatures inevitably tend to favor degradation processes, that lead to the formation of other products that we have not managed to detect (undetected).

Con formato: Resaltar

Table 2. Effect of reaction temperature and PMHS and FUR dosages on the hydrogenation of FUR for $1PdAl_2O_3$ and $1PdSiO_2$ catalysts [a]

Entry	Catalyst	PMHS (μL)	FUR (μL)	Conversion (%)	Yield (%)			
					FOL	THFA	MF	Undetected

1	$1PdAl_2O_3$	180	96	100	80.4	3.0	0	16.6
2		360	96	100	77.1	1.1	0	21.8
3		180	288	72.8	23.9	0	0	48.9
4*		180	96	99.6	62.9	3.0	0.7	33.0
6	$1PdSiO_2$	180	96	100	66.4	8.0	12.0	13.6
7		360	96	100	45.2	10.8	2.9	41.1
8		180	288	86.3	23.6	0	0	62.7
9*		180	96	97.7	56.9	5.2	6.9	28.7

[a] Experimental conditions: FUR (96 μL - 288 μL equivalent to 1.16 mmol – 3.48 mmol), PMHS (180 μL – 360 μL), supported Pd catalyst (50 mg), ethanol (5 mL), 303 K, 30 min. * 333 K

Con formato: Interlineado: sencillo

The effect of the amount of FUR initially fed has also been studied (**Table 2, entries 1, 3, 6 and 8**). Increasing the amount of FUR from 96 μL to 288 μL (from 1.16 mmol to 3.48 mmol FUR) caused a decrease in FUR conversion for both catalysts, from complete conversion to 72.8% and 86.3% for $1PdAl_2O_3$ and $1PdSiO_2$, respectively. The only reaction product obtained by increasing the amount of FUR was FOL with a very low yield for both catalysts (around 23%), but the most remarkable fact was the high percentage of undetected, which reached 62.7% for the $1PdSiO_2$ catalyst. This fact seems to confirm that PMHS reacts with FUR, as confirmed by GC-MS studies, since an increase in the FUR dosage causes a higher yield of undetected products.

Comentado [RMT7]: ¿Se sabe que se puede formar?

Finally, the effect of PMHS dosage on the catalytic performance was also studied (**Table 2, entries 1, 2, 6 and 7**). Full conversion of FUR was achieved for both catalysts at any PMHS dosage. The $1PdAl_2O_3$ catalyst showed a slight decrease in FOL yield from 80.4% to 77.1%, when the amount of PMHS was increased from 180 μL to 360 μL and the undetected products also increased from 16.6% to 21.8% (**Table 2, entries 1 and 2**).

The catalyst based on SiO_2 ($1PdSiO_2$) showed a more pronounced decrease in the FOL yield (from 66.4% to 45.2%) and also in the MF yield, but the most striking fact was the increase in the percentage of undetected products from 13.6% to 41.1% (**Table 2, entries 6 and 7**). This fact once again confirms the interaction of FUR and/or some reaction products with PMHS.

This study was also carried out using $2.5PdAl_2O_3$, which, as previously indicated, showed a different selectivity pattern (**Figure 3**), allowing us to elucidate the evolution of different products with the amount of PMHS added to the reaction media. As can be seen, by increasing the amount of PMHS from 180 µL to 360 µL, the conversion of FUR remains complete, but the selectivity profile changes, as expected, towards the formation of more hydrogenated products. Thus, FUR and FOL are completely hydrogenated to THFA, in fact, when the amount of PMHS was increased to 360 µL, FOL was not detected and a significant increase in the yield to THFA was observed (from 19.6% to 50.7%). Similarly, hydrogenation of the MF ring occurred, which was not detected by adding 360 µL PMHS, and the yield of MTHF increased from 1.5% to 18.8%.

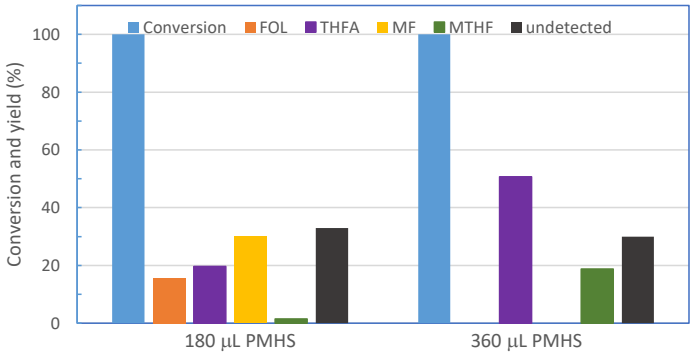

Figure 3. Effect of PMHS dosage on the hydrogenation of FUR over $2.5PdAl_2O_3$.

Comentado [RMT8]: Si se aumenta la Conc de FUR se dice que aumenta los no detectados por reacción del FUR con el PHMS pero si se aumenta la concentración de PHMS ¿no se favorecería también la reacción del FUR con el PHMS?

Con formato: Resaltar

Con formato: Resaltar

Experimental conditions: FUR (96 μL, 1.16 mmol), PMHS (180 μL or 360 μL), 2.5PdAl$_2$O$_3$ (50 mg), ethanol (5 mL), 303 K, 30 min.

These experiments demonstrated the versatility of this catalytic system, since the selectivity towards different reaction products can be modulated according to different parameters, such as Pd content, nature of the support, reaction temperature and PMHS dosage.

These experiments demonstrated the versatility of this catalytic system, since the selectivity towards different reaction products can be modulated according to different parameters, such as Pd content, nature of the support, reaction temperature and PMHS dosage.

In term of productivity, expressed as gram of target product formed per gram of catalyst per hour, the 1PdAl$_2$O$_3$ catalyst allows to reach a value of 397 mol_{FOL} mol_{Pd}^{-1} h^{-1} (Turnover frequency, TOF, of 397 h^{-1}) at 303 K after only 30 minutes, with 180 μL of PMHS (**Table 2, entry 1**), while using 2.5PdAl$_2$O$_3$ with 360 μL of PMHS, under similar experimental conditions, 100 mol_{THFA} mol_{Pd}^{-1} h^{-1} (TOF of 100 h^{-1}) (**Figure 3**). These values are much higher than those reported by Li et al.[32] (1-3.2 h^{-1}), using 0.5 mmol FUR, 0.1 g PMHS, 2 mol% Pd, 5 mol% chlorobenzene (PhCl), 1.5 mL n-butanol, 373 K after 2 h, but using more benign experimental conditions, with ethanol as solvent and without addition of PhCl.

Con formato: Fuente: Sin Cursiva

Catalyst characterization. Figure 4 shows the X-ray diffraction patterns of the catalysts with 1 wt% Pd loading on different supports. The basic support is formed by large MgO nanoparticles, as inferred from the presence of strong diffraction peaks at 2θ (º) = 37, 43 and 62, corresponding to (111), (002) and (202) planes (JCPDS No. 87-0653). The

presence of the cubic γ-Al_2O_3 was identified for the *x*$PdAl_2O_3$ catalysts (PDF 01-077-0396), with diffraction peaks at 2θ (º) = 37.4, 39.6, 45.8, 60.3 and 67.4. No visible diffractions peaks due to PdO were observed, so PdO was highly dispersed on this support. As for the *x*$PdSiO_2$ catalyst, a broad diffraction band centered at 2θ (°) = 21.6, characteristic of amorphous SiO_2, was identified in its diffractograms, although the catalysts with higher Pd content (2.5% and 5 wt%) show a new diffraction signal at 2θ(º)= 33.8, which can be attributed to PdO (PDF: 00-048-0074) **(Figure S1)**. This last band is more intense for higher Pd loading. This would indicate an increase in the average particle size of the PdO crystallites as the metallic loading on the catalyst increases. However, when alumina was used as support, a higher dispersion was obtained for the same percentage of Pd incorporated into the catalyst.

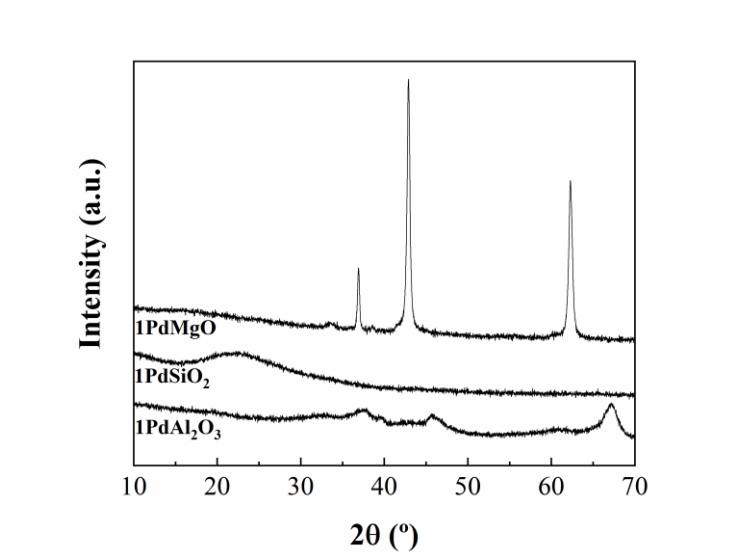

Figure 4. X-ray diffraction patterns of supported Pd catalysts with 1 wt% Pd.

The morphology of catalysts was studied by transmission electron microscopy, and the images are shown in **Figure 5**. Catalysts consist of aggregates of small particles, with no

areas of particles with well-defined shapes. These data are consistent with the low crystallinity inferred from XRD data (**Figure 4**). The EDX analysis shows a good dispersion of the different chemical elements, and, in all cases, homogeneous distributions of PdO particles smaller than 15 nm were observed.

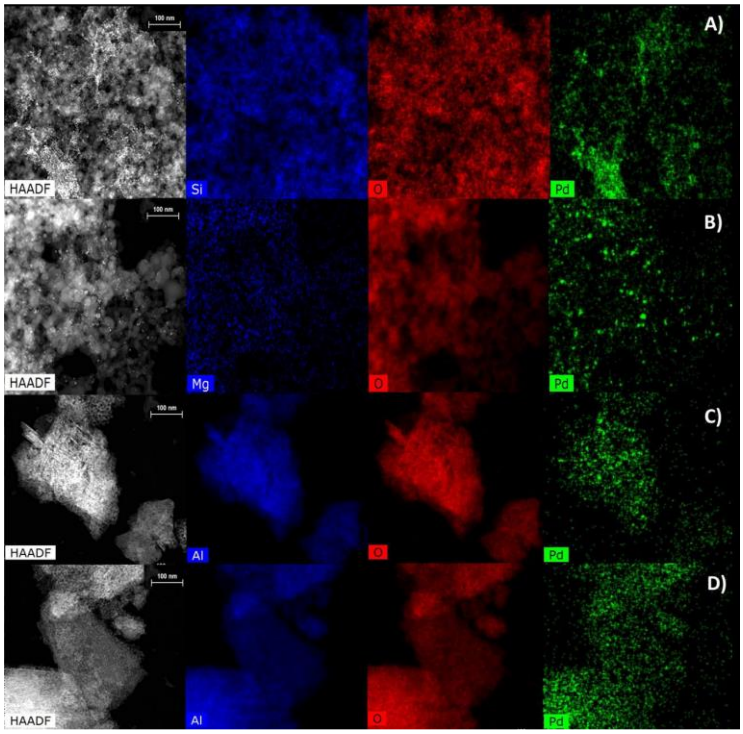

Figure 5. TEM micrographs and EDX analysis for: A) 1PdSiO$_2$, B) 1PdMgO, C) 1PdAl$_2$O$_3$ and D) 2.5PdAl$_2$O$_3$

The textural properties of supported Pd catalysts with 1 wt% Pd, and those supported on Al$_2$O$_3$ and SiO$_2$ with different Pd loadings were determined by N$_2$ adsorption-desorption isotherms 77 K (**Figures 6 and S2**). Their textural data are sumarized in **Table 3**. According to the IUPAC classification[36] the isotherms of the *x*PdAl$_2$O$_3$ catalysts are

Type IV with a H2-shaped hyteresis loop, which is typical for mesoporous materials. The textural parameters (BET surface area, pore volume and pore size distribution) did not show any significant change with Pd loading due to the low Pd loading. *x*PdSiO$_2$ catalysts showed Type II isotherms, which are characteristic to macroporous materials with significant N_2 adsorption at high relative pressure due to interparticle voids between SiO_2 particles. In the case of 1PdMgO, the worst textural properties agree well with its high crystallinity, as inferred from XRD data.

Table 3. Textural properties of *x*PdAl$_2$O$_3$ and xPSiO$_2$ catalysts

Sample	BET Surface Area ($m^2 \cdot g^{-1}$)	V_p ($cm^3 \cdot g^{-1}$)
1PdAl$_2$O$_3$	136	0.221
2.5PdAl$_2$O$_3$	137	0.218
5PdAl$_2$O$_3$	131	0.213
1PdSiO$_2$	173	0.482
2.5PdSiO$_2$	185	0.453
5PdSiO$_2$	190	0.553
1PdMgO	13	0.021

A slight increase in BET surface area with Pd content (**Table 3**) was observed for *x*PdSiO$_2$ catalysts, which may be related to interparticle voids between large palladium oxide nanoparticles. The pore size distributions (**Figures 7 and S3**) were estimated by density functional theory (DFT). The *x*PdAl$_2$O$_3$ catalysts showed a narrow pore size distribution with similar pore diameter for materials with different Pd loading, with a maximum centered at 5.9 nm. Larger and more heterogeneous pore sizes were obtained

for the *x*PdSiO$_2$ catalysts, whereas the non-porous nature of 1PdMgO can be inferred from its corresponding pore size distribution.

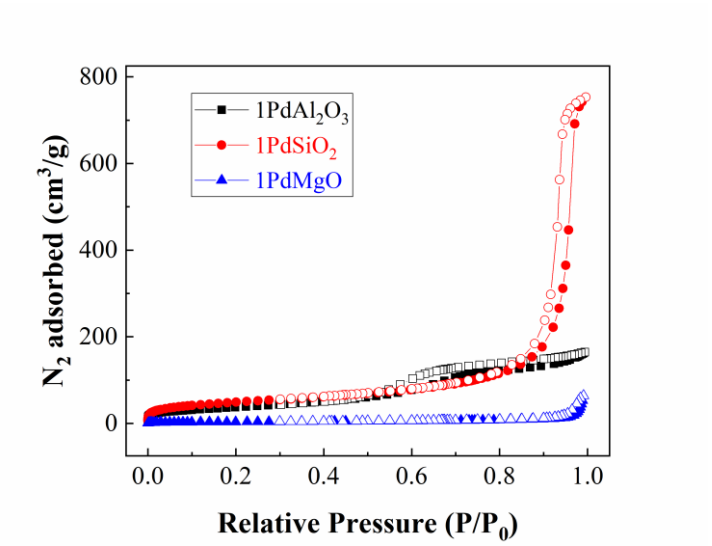

Figure 6. N_2 adsorption–desorption isotherm at 77 K of supported Pd catalysts with 1 wt% Pd loading.

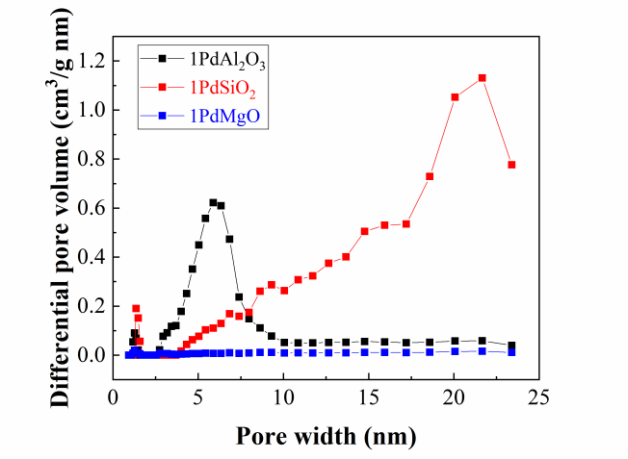

Figure 7. Pore size distribution (estimated from DFT method) of supported Pd catalysts with 1 wt% Pd.

X-ray photoelectron spectroscopy (XPS) was performed to obtain further information on the oxidation state of Pd and the surface chemical composition of fresh and used catalysts. The XPS data are shown in Table 4. Binding energies (BE) of Al 2p, Mg 2p and Si 2p are characteristics of the corresponding oxides, which hardly vary after the incorporation of Pd species.[42]

X-ray photoelectron spectroscopy (XPS) was performed to obtain further information on the oxidation state of Pd and the surface chemical composition of fresh and used catalysts. The XPS data are shown in Table 4. Binding energies (BE) of Al 2p, Mg 2p and Si 2p are characteristics of the corresponding oxides, which hardly vary after the incorporation of Pd species.[42]

Table 4. XPS data of fresh and used Pd-based catalysts (1 wt% Pd loading).

Catalyst	Binding Energy, eV (Atomic Concentration, %)						Pd/M Atomic Ratio
	C 1s	O 1s	Mg 2p	Al 2p	Si 2p	Pd $3d_{5/2}$	
1PdMgO	284.8 (12.2)	532.7 (23.0) 530.6 (23.7) → 50,82	50.2 (36.8)	-	-	336.7 (0.22)	0.006
1PdMgO-U	284.8 (39.9)	532.7 (29.9)	49.9 (13.9)	-	103.3 (6.3)	336.6 (0.44)	0.032

		530.6 (19.7)					
$1PdAl_2O_3$	284.8 (9.1)	530.8 (61.3)	-	74.1 (29.5)	-	335.9 (0.16)	0.004
$1PdAl_2O_3$-U	284.8 (28.0)	530.8 (45.3)	-	74.1 (19.6)	103.3 (7.0)	335.2 (0.14)	0.007
$1PdSiO_2$	284.8 (3.5)	532.8 (67.3)	-	-	103.5 (29.2)	336.1 (0.04)	0.001
$1PdSiO_2$-U	284.8 (5.9)	532.7 (61.0)	-	-	103.4 (33.2)	334.8 (0.31)	0.009

The Pd 3d core level spectra of catalysts with 1 wt% Pd are shown in **Figure 8**. Pd species in fresh catalysts are mainly present as PdO, whose BE is between 335.9 eV and 336.7 eV (Pd $3d_{5/2}$). Regarding the surface M/O atomic ratio, they differ from that of the theoretical values of supports (Al_2O_3, SiO_2 and MgO), mainly in the case of MgO and Al_2O_3. This can be explained by the easy carbonation of MgO and the hydroxylation of the surface of Al_2O_3 surface, which lead to a higher proportion of surface species.

Con formato: Subíndice

Con formato: Subíndice

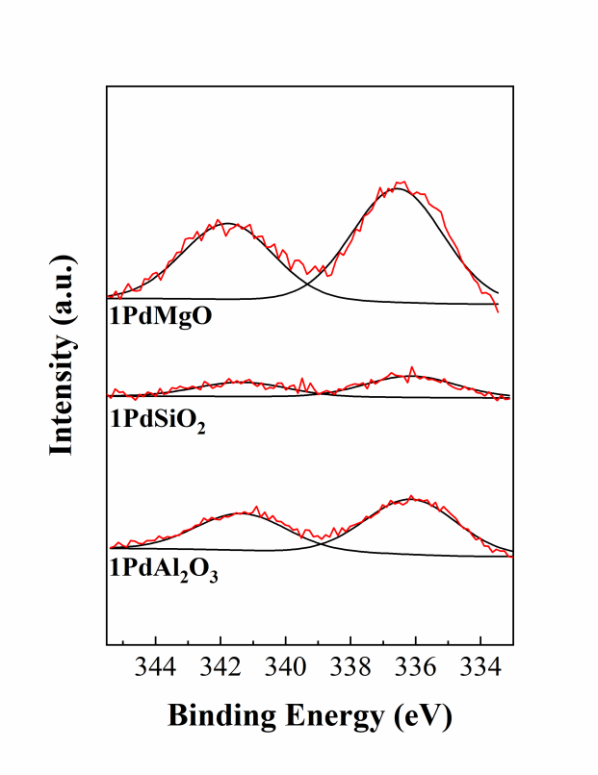

Figure 8. Pd 3d core level spectra of supported Pd catalysts with 1 wt% Pd.

The atomic percentage of Pd on the catalyst surface is very low in the case of $1PdSiO_2$ (0.04 at%), which is consistent with the formation of large PdO nanoparticles, as inferred from the XRD data (**Figure 4**). However, after the catalytic test (303 K for 30 min), Pd is mainly as metallic nanoparticles (Pd $3d_{5/2}$ BE: 334.8-335.2 eV), due to the reduction in the reaction medium by the presence of PMHS (**Figure 9**).

Comentado [RMT9]: Consumo de H por el Pd….¿La cantidad de PHMS es estequiométrica o está siempre en exceso?

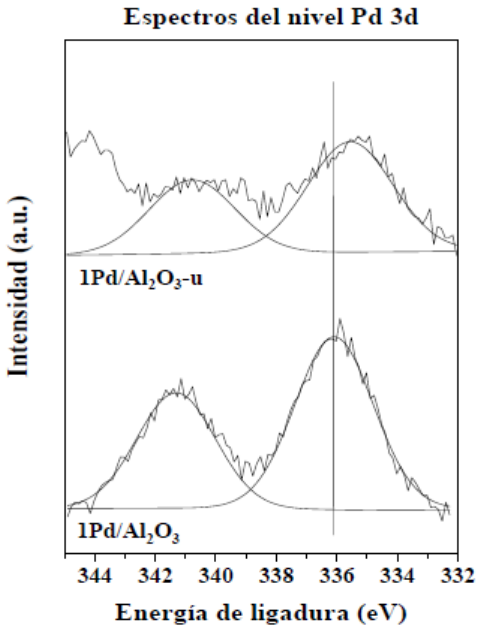

Figura 9. Espectro XPS obtenido del 1%Pd/Al_2O_3 usado (superior) y fresco (inferior)

Comentado [RMT10]: La letra del caption no es Times New Roman y está en español

Also noteworthy is the presence of siliceous species on the catalyst surface after the catalytic test, with BE values (100.2 eV) lower than those corresponding to silica (103.2 eV), which can be explained by the deposition of siliceous species derived from PMHS. In addition, a slight increase in Si surface area is observed in the 1PdSiO_2 catalyst. Regarding the carbon content, the Al_2O_3-based catalyst showed a significant increase after the reaction, which could be explained by the adsorption of reaction products (undetected), as well as the carbon associated with PMHS derivatives bound to the heterogeneous catalysts.

We are working in the discussion of catalytic data considering the physico-chemical properties of catalysts, and then we will prepare the conclusions.

CONCLUSION

The present work has demonstrated that Pd-based catalysts with very low loading of Pd (1 wt%) are active and selective catalysts for the reduction of FUR, using polymethylhydroxysiloxane (PMHS) as reducing agent as alternative to hydrogen gas or alcohols as hydrogen donors. PMHS, a polymeric waste product of the silicone industry, is a non-toxic and sustainable reductant, stable in water/air and soluble in most organic solvents. Although all catalysts tested are catalytically active, those supported on Al_2O_3 and SiO_2 showed complete conversion after 30 min of reaction at 303 K, whereas a 27.7% was attained using MgO. $1PdAl_2O_3$ (1 wt% Pd) catalyst was initially very selective to furfuryl alcohol (80.4% yield of FOL), which was hydrogenated to tetrahydrofurfuryl alcohol (THFA) at longer reaction times, or by increasing both the amount of PMHS and Pd loading. Using the $1PdAl_2O_3$ catalyst, a TOF value of 397 $mol_{FOL}\ mol_{Pd}^{-1}\ h^{-1}$ at 303 K after only 30 minutes was obtained, with only 180 μL of PMHS in ethanol, as solvent, while increasing both the amount of Pd to 2.5 wt% ($2.5PdAl_2O_3$) and that of PMHS until 360 μL, under similar experimental conditions, 100 $mol_{THFA}\ mol_{Pd}^{-1}\ h^{-1}$ can be produced. This suitable catalytic performance can be explained due to the high surface area of the support (Al_2O_3)……

CRediT authorship contribution statement

M. Esther Medina-Ruiz, Rocío Maderuelo-Solera, Carmen P. Jiménez-Gómez: Investigation. Irene Malpartida, Cristina García-Sancho: Supervision. Christophe Len, Josefa M. Mérida-Robles, Juan A. Cecilia, Ramón Moreno-Tost, Pedro Maireles-Torres: Supervision. Ramón Moreno-Tost, Pedro Maireles-Torres: Project Administration, Funding Acquisition. Christophe Len, Josefa M. Mérida-Robles, Pedro Maireles-Torres: Writing, Review and Editing (final draft).

Conflicts of interest

The authors declare that they have no known competing financial interests or personal relationships that could have appeared to influence this work.

Author information

Corresponding Authors: Christophe Len: Josefa M. Mérida-Robles: jmerida@uma.es

Acknowledgements

This research was funded by Spanish Ministry of Science and Innovation (PID2021-122736OB-C42) and FEDER (European Union) funds.

References

(1) García-Sancho, C.; Cecilia, J. A.; Luque, R. Conversion of Lignocellulosic Biomass to Biofuels. In *Heterogeneous Catalysts*; Wiley, 2021; pp 593–616.

(2) Gómez Millán, G.; Hellsten, S.; Llorca, J.; Luque, R.; Sixta, H.; Balu, A. M. Recent Advances in the Catalytic Production of Platform Chemicals from Holocellulosic Biomass. *ChemCatChem*. Wiley Blackwell April 18, 2019, pp 2022–2042. https://doi.org/10.1002/cctc.201801843.

(3) Mariscal, R.; Maireles-Torres, P.; Ojeda, M.; Sádaba, I.; López Granados, M. Furfural: A Renewable and Versatile Platform Molecule for the Synthesis of Chemicals and Fuels. *Energy Environ. Sci.* **2016**, *9* (4), 1144–1189. https://doi.org/10.1039/C5EE02666K.

(4) Khemthong, P.; Yimsukanan, C.; Narkkun, T.; Srifa, A.; Witoon, T.; Pongchaiphol, S.; Kiatphuengporn, S.; Faungnawakij, K. Advances in Catalytic Production of Value-Added Biochemicals and Biofuels via Furfural Platform Derived Lignocellulosic Biomass. *Biomass and Bioenergy*. Elsevier Ltd May 1, 2021. https://doi.org/10.1016/j.biombioe.2021.106033.

(5) Xu, C.; Paone, E.; Rodríguez-Padrón, D.; Luque, R.; Mauriello, F. Recent Catalytic Routes for the Preparation and the Upgrading of Biomass Derived Furfural and 5-Hydroxymethylfurfural. *Chem Soc Rev* **2020**, *49* (13), 4273–4306. https://doi.org/10.1039/d0cs00041h.

(6) Richel, A.; Maireles-Torres, P.; Len, C. Recent Advances in Continuous Reduction of Furfural to Added Value Chemicals. *Current Opinion in Green and Sustainable Chemistry*. Elsevier B.V. October 1, 2022. https://doi.org/10.1016/j.cogsc.2022.100655.

(7) Wang, Y.; Zhao, D.; Rodríguez-Padrón, D.; Len, C. Recent Advances in Catalytic Hydrogenation of Furfural. *Catalysts*. MDPI October 1, 2019. https://doi.org/10.3390/catal9100796.

(8) Mandalika, A.; Qin, L.; Sato, T. K.; Runge, T. Integrated Biorefinery Model Based on Production of Furans Using Open-Ended High Yield Processes. *Green Chemistry* **2014**, *16* (5), 2480–2489. https://doi.org/10.1039/c3gc42424c.

(9) Iroegbu, A. O.; Hlangothi, S. P. Furfuryl Alcohol a Versatile, Eco-Sustainable Compound in Perspective. *Chem. Africa* **2019**, *2019*, 223–239.

(10) González Maldonado, G. M.; Assary, R. S.; Dumesic, J.; Curtiss, L. A. Experimental and Theoretical Studies of the Acid-Catalyzed Conversion of Furfuryl Alcohol to Levulinic Acid in Aqueous Solution. *Energy Environ Sci* **2012**, *5* (5), 6981–6989. https://doi.org/10.1039/c2ee03465d.

(11) Onkarappa, S. B.; Bhat, N. S.; Dutta, S. Preparation of Alkyl Levulinates from Biomass-Derived 5-(Halomethyl)Furfural (X = Cl, Br), Furfuryl Alcohol, and Angelica Lactone Using Silica-Supported Perchloric Acid as a Heterogeneous Acid Catalyst. *Biomass Convers. Biorefinery* **2020**, *10*, 849–856.

(12) Chaffey, D. R.; Davies, T. E.; Taylor, S. H.; Graham, A. E. Etherification Reactions of Furfuryl Alcohol in the Presence of Orthoesters and Ketals: Application to the Synthesis of Furfuryl Ether Biofuels. *ACS Sustain Chem Eng* **2018**, *6* (4), 4996–5002. https://doi.org/10.1021/acssuschemeng.7b04636.
(13) Merat, N.; Godawa, C.; Gaset, A. High Selective Production of Tetrahydrofurfuryl Alcohol: Catalytic Hydrogenation of Furfural and Furfuryl Alcohol. *J. Chem. Technol. Biotechnol.* **2007**, *48*, 145–159.
(14) Zhang, B.; Zhu, Y.; Ding, G.; Zheng, H.; Li, Y. Selective Conversion of Furfuryl Alcohol to 1,2-Pentanediol over a Ru/MnOx Catalyst in Aqueous Phase. *Green Chem.* **2012**, *14*, 3402.
(15) Hu, L.; Zhao, G.; Hao, W.; Tang, X.; Sun, Y.; Lin, L.; Liu, S. Catalytic Conversion of Biomass-Derived Carbohydrates into Fuels and Chemicals via Furanic Aldehydes. *RSC Advances*. November 28, 2012, pp 11184–11206. https://doi.org/10.1039/c2ra21811a.
(16) Hronec, M.; Fulajtárova, K.; Mičušik, M. Influence of Furanic Polymers on Selectivity of Furfural Rearrangement to Cyclopentanone. *Appl Catal A Gen* **2013**, *468*, 426–431. https://doi.org/10.1016/j.apcata.2013.08.052.
(17) Chen, S.; Wojcieszak, R.; Dumeignil, F.; Marceau, E.; Royer, S. How Catalysts and Experimental Conditions Determine the Selective Hydroconversion of Furfural and 5-Hydroxymethylfurfural. *Chemical Reviews*. American Chemical Society November 28, 2018, pp 11023–11117. https://doi.org/10.1021/acs.chemrev.8b00134.
(18) Wang, Y.; Zhao, D.; Liang, R.; Triantafyllidis, K. S.; Yang, W.; Len, C. Transfer Hydrogenation of Furfural to Furfuryl Alcohol over Modified Zr-Based Catalysts Using Primary Alcohols as H-Donors. *Molecular Catalysis* **2021**, *499*. https://doi.org/10.1016/j.mcat.2020.111199.
(19) Wang, Y.; Prinsen, P.; Triantafyllidis, K.; Karakoulia, S. A.; Yepez, A.; Len, C. Batch versus Continuous Flow Performance of Supported Mono- and Bimetallic Nickel Catalysts for Catalytic Transfer Hydrogenation of Furfural in Isopropanol. *ChemCatChem* **2018**, *10* (16), 3459–3468.
(20) Long, J.; Xu, Y.; Zhao, W.; Li, H.; Yang, S. Heterogeneous Catalytic Upgrading of Biofuranic Aldehydes to Alcohols. *Frontiers in Chemistry*. Frontiers Media S.A. July 26, 2019. https://doi.org/10.3389/fchem.2019.00529.
(21) Wang, C.; Guo, Z.; Yang, Y.; Chang, J.; Borgna, A. Hydrogenation of Furfural as Model Reaction of Bio-Oil Stabilization under Mild Conditions Using Multiwalled Carbon Nanotube (MWNT)-Supported Pt Catalysts. *Ind. Eng. Chem. Res.* **2014**, *53*, 11284–11291.
(22) Johnson, T. C.; Morris, D. J.; Wills, M. Hydrogen Generation from Formic Acid and Alcohols Using Homogeneous Catalysts. *Chem Soc Rev* **2010**, *39* (1), 81–88. https://doi.org/10.1039/b904495g.
(23) Valentini, F.; Kozell, V.; Petrucci, C.; Marrocchi, A.; Gu, Y.; Gelman, D.; Vaccaro, L. Formic Acid, a Biomass-Derived Source of Energy and Hydrogen for Biomass Upgrading. *Energy Environ Sci* **2019**, *12* (9), 2646–2664. https://doi.org/10.1039/c9ee01747j.
(24) Du, J.; Zhang, J.; Sun, Y.; Jia, W.; Si, Z.; Gao, H.; Tang, X.; Zeng, X.; Lei, T.; Liu, S.; Lin, L. Catalytic Transfer Hydrogenation of Biomass-Derived Furfural to Furfuryl Alcohol over in-Situ Prepared Nano Cu-Pd/C Catalyst Using Formic Acid as Hydrogen Source. *J Catal* **2018**, *368*, 69–78. https://doi.org/10.1016/j.jcat.2018.09.025.
(25) Nagaiah, P.; Gidyonu, P.; Ashokraju, M.; Rao, M. V.; Challa, P.; Burri, D. R.; Kamaraju, S. R. R. Magnesium Aluminate Supported Cu Catalyst for Selective Transfer Hydrogenation of Biomass Derived Furfural to Furfuryl Alcohol with Formic Acid as Hydrogen Donor. *ChemistrySelect* **2019**, *4*, 145–151.
(26) Lawrence, N. J.; Drew, M. D.; Bushell, S. M. *Polymethylhydrosiloxane: A Versatile Reducing Agent for Organic Synthesis*; 1999.
(27) Wu, W.; Zhao, W.; Fang, C.; Wang, Z.; Yang, T.; Li, H.; Yang, S. Quantitative Hydrogenation of Furfural to Furfuryl Alcohol with Recyclable KF and Hydrosilane at Room Temperature in Minutes. *Catal Commun* **2018**, *105*, 6–10. https://doi.org/10.1016/j.catcom.2017.11.005.
(28) Zhao, W.; Wu, W.; Li, H.; Fang, C.; Yang, T.; Wang, Z.; He, C.; Yang, S. Quantitative Synthesis of 2,5-Bis(Hydroxymethyl)Furan from Biomass-Derived 5-Hydroxymethylfurfural and Sugars over Reusable Solid Catalysts at Low Temperatures. *Fuel* **2018**, *217*, 365–369. https://doi.org/10.1016/j.fuel.2017.12.069.
(29) Yu, Z.; Wu, W.; Li, H.; Yang, S. Highly Selective Reduction of Bio-Based Furfural to Furfuryl Alcohol Catalyzed by Supported KF with Polymethylhydrosiloxane (PMHS). *J Chem* **2020**, *2020*. https://doi.org/10.1155/2020/4809127.
(30) Long, J.; Zhao, W.; Xu, Y.; Wu, W.; Fang, C.; Li, H.; Yang, S. Low-Temperature Catalytic Hydrogenation of Bio-Based Furfural and Relevant Aldehydes Using Cesium Carbonate and Hydrosiloxane. *RSC Adv* **2019**, *9* (6), 3063–3071. https://doi.org/10.1039/c8ra08616h.

(31) Yu, Z.; Xu, F.; Li, Y.; Konno, H.; Li, H.; Yang, S. Tetraethylammonium Fluoride-Mediated A Green Hydrogen Transfer Process for Selective Reduction of Biomass-Derived Aldehydes. *Current Green Chemistry* **2019**, *6* (2), 127–134. https://doi.org/10.2174/2213346106666190830115519.
(32) Li, H.; Zhao, W.; Saravanamurugan, S.; Dai, W.; He, J.; Meier, S.; Yang, S.; Riisager, A. Control of Selectivity in Hydrosilane-Promoted Heterogeneous Palladium-Catalysed Reduction of Furfural and Aromatic Carboxides. *Commun Chem* **2018**, *1* (1). https://doi.org/10.1038/s42004-018-0033-z.
(33) Li, H.; Zhao, W.; Fang, Z. Hydrophobic Pd Nanocatalysts for One-Pot and High-Yield Production of Liquid Furanic Biofuels at Low Temperatures. *Appl Catal B* **2017**, *215*, 18–27. https://doi.org/10.1016/j.apcatb.2017.05.039.
(34) Ding, W.; Li, H.; Zong, R.; Jiang, J.; Tang, X. Controlled Hydrodeoxygenation of Biobased Ketones and Aldehydes over an Alloyed Pd-Zr Catalyst under Mild Conditions. *ACS Sustain Chem Eng* **2021**, *9* (9), 3498–3508. https://doi.org/10.1021/acssuschemeng.0c07805.
(35) Williamson, G. K.; Hall, W. H. X-Ray line broadening from filed aluminium and wolfram,. *Acta Metallurgica* **1953**, *1*, 22-31.
(36) Brunauer, S.; Emmett, P. H.; Teller, E. *Adsorption of Gases in Multimolecular Layers*; 1938. https://pubs.acs.org/sharingguidelines.
(37) Landers, J.; Gor, G. Y.; Neimark, A. V. Density Functional Theory Methods for Characterization of Porous Materials. *Colloids Surf A Physicochem Eng Asp* **2013**, *437*, 3–32. https://doi.org/10.1016/j.colsurfa.2013.01.007.
(38) Wang, Z.; Wang, X.; Zhang, C.; Arai, M.; Zhou, L.; Zhao, F. Selective Hydrogenation of Furfural to Furfuryl Alcohol over Pd/TiH2 Catalyst. *Molecular Catalysis* **2021**, *508*. https://doi.org/10.1016/j.mcat.2021.111599.
(39) Merlo, A. B.; Vetere, V.; Ruggera, J. F.; Casella, M. L. Bimetallic PtSn Catalyst for the Selective Hydrogenation of Furfural to Furfuryl Alcohol in Liquid-Phase. *Catal Commun* **2009**, *10* (13), 1665–1669. https://doi.org/10.1016/j.catcom.2009.05.005.
(40) Albilali, R.; Douthwaite, M.; He, Q.; Taylor, S. H. The Selective Hydrogenation of Furfural over Supported Palladium Nanoparticle Catalysts Prepared by Sol-Immobilisation: Effect of Catalyst Support and Reaction Conditions. *Catal Sci Technol* **2018**, *8*, 252–267. https://doi.org/10.1039/c7cy02110k.
(41) O'Driscoll; Leahy, J. J.; Curtin, T. The Influence of Metal Selection on Catalyst Activity for the Liquid Phase Hydrogenation of Furfural to Furfuryl Alcohol. *Catal Today* **2017**, *279*, 194–201. https://doi.org/10.1016/j.cattod.2016.06.013.
(42) Moulder, J. F.; Stickle, W. F.; Sobol, P. E. '; Bomben, K. D.; Chastain, J. *Handbook of X-Ray Photoelectron Spectroscopy AReference Book of Standard Spectra for Identification and Interpretation of XPS Data*.

SUPPLEMENTARY INFORMATION

Supported Palladium Catalysts for the Conversion of Furfural with Polymethylhydrosiloxane

M. Esther Medina Ruiz,[†] Rocío Maderuelo-Solera,[†] Carmen P. Jiménez-Gómez,[†] Ramón Moreno-Tost,[†] Irene Malpartida,[‡] Cristina García-Sancho,[†] Juan Antonio Cecilia,[†] Christophe Len,[§,||] Josefa M. Mérida-Robles,[†,*] Pedro Maireles-Torres,[†]

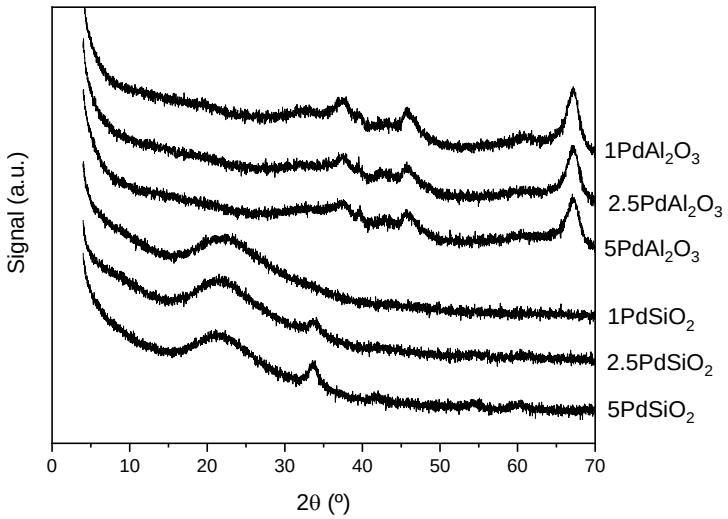

Figure S1. X-ray diffraction patterns of *x*$PdAl_2O_3$ and *x*$PdSiO_2$ catalysts with different Pd contents.

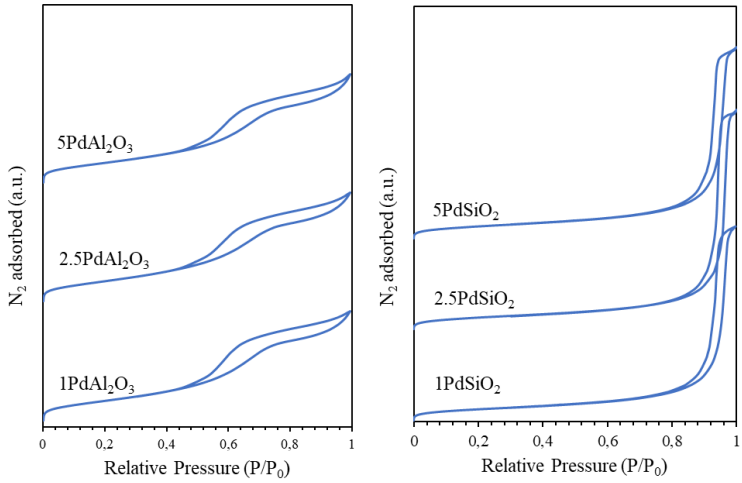

Figure S2. N_2 adsorption–desorption isotherm at 77 K of *x*$PdAl_2O_3$ and *x*$PSiO_2$ catalysts.

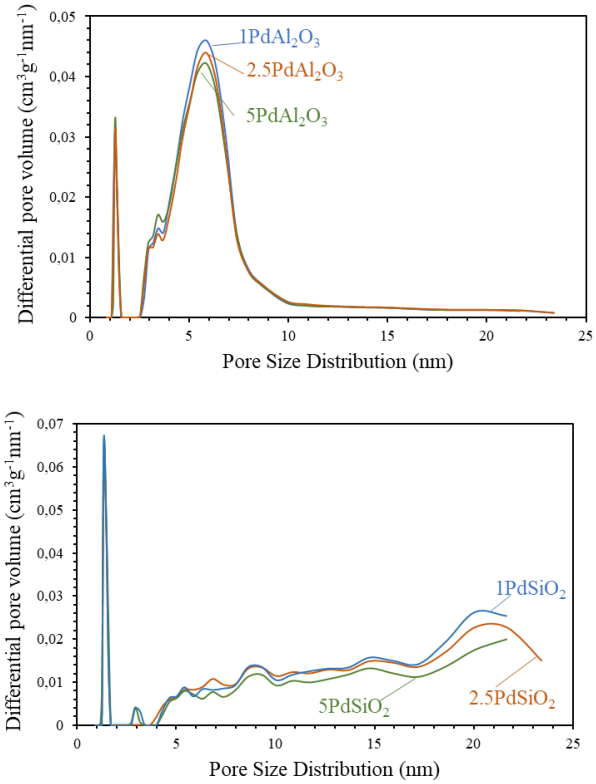

Figure S3. Pore size distribution (estimated from DFT method) of *x*$PdAl_2O_3$ and *x*$PSiO_2$ catalysts.